Full Title: **Mapping molecules to structure: unveiling secrets of centriole and cilia assembly with near-atomic resolution**

Short Title: **Secrets of centriole and cilia assembly**

Authors: Swadhin Chandra Jana*#, Gaëlle Marteil*#, Mónica Bettencourt-Dias*

***- corresponding authors; #-** these authors contributed equally

Affiliation: Instituto Gulbenkian de Ciência, Oeiras, Portugal.

e-mail correspondance:

Swadhin Chandra Jana sjana@igc.gulbenkian.pt

Gaëlle Marteil gmarteil@igc.gulbenkian.pt

Mónica Bettencourt-Dias mdias@igc.gulbenkian.pt

Abstract

Centrioles are microtubule (MT)-based cylinders that form centrosomes and modified into basal bodies that template the axoneme, the ciliary MT skeleton. These MT-based structures are present in all branches of the eukaryotic tree of life, where they have important sensing, motility and cellular architecture-organising functions. Moreover, they are altered in several human conditions and diseases, including sterility, ciliopathies and cancer. Although the ultrastructure of centrioles and derived organelles has been known for over 50 years, the molecular basis of their remarkably conserved properties, such as their 9-fold symmetry, has only now started to be unveiled. Recent advances in imaging, proteomics and crystallography, allowed the building of 3D models of centrioles and derived structures with unprecedented molecular details, leading to a much better understanding of their assembly and function. Here, we cover progress in this field, focusing on the mechanisms of centriole and cilia assembly.

Introduction

Centrioles and Basal Bodies are analogous MT-based organelles essential for the formation of centrosomes and cilia, respectively [1]. The term “centriole” is typically used when the centriole is within the centrosome and “basal body” (BB) when docked to the membrane. For simplicity, we will refer to these structures as Centriole/Basal Body (CBB) hereafter. Centrosomes are made of two centrioles and pericentriolar material that nucleate and anchor cytoplasmic MTs. Cilia are MT-based motile or immotile protrusions that grow from the distal end of BBs. The “canonical” CBB is a ~500nm long and 250nm wide cylinder, composed of 9 radially symmetric triplet MTs (Figure 1A), showing a proximo-distal polarity. CBBs can also display variations in their structures, albeit more rarely, with the presence of doublet and singlet MTs in *Drosophila* somatic cells and *C.elegans*, respectively [2]. At the proximal end of most CBBs there is a cartwheel [3-5], a structure typically comprised of a 20-25 nm diameter central hub from which 9 radial spokes emanate to contact the MTs. In contrast, *C. elegans* centriole consists of a 60 nm diameter central tube surrounded by the MT without a well-defined hub (Figure 1B, [6]). At their distal end, human centrioles are composed of 9 radially symmetric doublet MTs and appendages, sub-distal and distal, which play important roles in anchoring MTs and in docking centrioles to the membrane to form cilia, respectively [1]. Periodic structures have also been

described in the lumen of centrioles at their distal part [7,8]. Upon centriole conversion to BBs, centrioles gain a new structure at their distal end, the transition zone (TZ). At the TZ the doublet MTs are heavily cross-linked to the surrounding ciliary membrane and the TZ may act as a gatekeeper for material that goes into cilia [1,9]. The doublet MTs of the TZ are thought to template the MT skeleton of the cilium, also called axoneme, which consequently exhibits a 9-fold symmetry.

All structures described above were initially studied using conventional transmission electron microscopy. Their remarkable features and conservation in evolution led to speculations on their functions. For example, the cartwheel's 9-fold symmetry and its presence in early stage of centriole assembly suggest it helps establishing the conserved centriole 9-fold symmetry. However, in part due to the small size of those structures, experimental tests of those hypotheses only became possible recently. New insights on CBB and cilia assembly and function are emerging from studies using modern techniques, such as genome wide RNAi screens, sensitive proteomics, X-ray crystallography, comparative genomics, super-resolution light microscopy and cryo-electron tomography. We will discuss how the new data is addressing old questions.

Centriole components and their organization

Procentrioles form close to already existing centrioles in most species, with the cartwheel forming early. In human cultured cells the cartwheel disassembles during mitosis, while it is generally maintained in cells that form motile cilia [2,10,11]+Alvey R. 1986+ Gonczy 2007. Recent studies identified mutants showing impaired cartwheel formation and/or stability in *Chlamydomonas*, *Drosophila* and *Tetrahymena* [12-14]. Those mutants show CBBs and/or axonemes with aberrant symmetry [12,13], abnormally disengaged centrioles and BBs that disassemble upon cilia beating [14]. Collectively, these data suggest the cartwheel plays a variety of functions such as helping to establish the 9-fold symmetry, keeping centrioles linked and stabilising them as BBs of motile cilia. The mechanisms directing cartwheel assembly were only described recently. We next discuss the latest studies unravelling these mechanisms.

Cartwheel components and their organisation

The full architecture of the cartwheel was recently unveiled by subtomogram averaging and 9-fold symmetrisation, rendered possible by cleverly studying the very long BBs with long cartwheels (~1.5 µm) of *Trichonympha*, a protist that lives inside termites [15,16]. Several novel features were identified in the cartwheel: i) a 9-fold symmetric structure within the hub, ii) the periodic organization of the hub and the spokes and iii) the chiral symmetry of the pinhead, link between the spoke and the MT. In its central region, the 22 nm diameter central hub and the radial spokes exhibit a ~8.5 nm periodicity while, 20 nm far from the hub, two radial spokes merge into a single bundle, forming layers with a ~17 nm periodicity (Figure 1C, [15,16]) + gopalakhrishnan JBC ref. These radial spokes are symmetric, with a 40° rotation angle, indicating that the central hub is a lattice of stacked rings rather than a spiral. The pinhead, consisting of two structures: Pinbody and Pinfoot, is polarized along the proximal-distal CBB axis. This structure bridges radial spokes as well as A- and C- tubule of adjacent triplet MTs (Figure 1C, [16]). It is likely that these several novel structures identified within the proximal part of the centrioles play pivotal roles in centriole assembly, directionality for elongation and inherent chirality of the triplet MTs.

How is the cartwheel assembled? The earliest event in cartwheel assembly is likely to be the recruitment of Polo-like kinase 4 (PLK4), a master regulator of centriole biogenesis, on the surface of the proximal end of the mother centriole [17]. A distant orthologue of PLK4 (ZYG-1) [18] recruits SAS-6 to the proximal end of the mother centriole in *C. elegans* in a kinase activity independent manner suggesting that PLK4 may play a structural role at the onset of centriole biogenesis [19]+Jana 2012. SAS-6 localizes to the hub and its essential role in cartwheel formation is evolutionary conserved [12,20-22]. SAS-6 also contributes to the centriole 9-fold symmetry in *Drosophila,* zebrafish*, Chlamydomonas* and *C. elegans* [13,23,24]. Crystal structures and Cryo-Electron Micrographs of the N-terminus of SAS-6 show it self-assembles in ring-like oligomeric structures similar to the hub [23,24]. Additionally, SAS-6 coiled-coil domains can homo-dimerize to form a 30-50 nm long rod (Figure 1E). Both the observed diameter of the ring formed by SAS-6 *in vitro* and the rotation angle between two adjacent coiled-coil homodimers [23,24] are in accordance with the ultra-structural data of *Trichonympha* cartwheels [15,16]. These data support the structural model of a 9-fold symmetric cartwheel

composed of 9 N-terminal dimers of SAS-6 forming the hub, from which 9 coiled-coil SAS-6 dimers radiate to constitute the spokes (Figure 1C). Interestingly, the globular C-terminal domain of SAS-6 varies in size across different organisms (Figure 1E), suggesting diverse possible roles in radial spoke and pinhead assembly and/or maintenance. Further investigation on this domain's structure and roles in cartwheel formation/stability *in vivo* will be important.

Other molecules also play a role in cartwheel formation and connection to the MTs. The predicted maximum coiled-coil length of SAS-6 is much shorter than the radial distance between the cartwheel hub and the A-tubule of triplet MTs; thus SAS-6 coiled-coils cannot solely account for the entire spoke-pinhead length (Figure 1E) [15,24]. CEP135/BLD10 and/or CPAP/SAS-4 may act as the physical link between the cartwheel spokes and the MT triplets [25] and STIL/Ana2/SAS-5 may have important role in regulating this process [26]. CEP135/BLD10 localises at the periphery of the cartwheel studied by immuno- electron microscopy [27] and to the centriolar lumen and wall by super-resolution microscopy [28-30]. Moreover, the N- and C-termini of CEP135 directly bind to MTs and SAS-6 coiled-coils, respectively (Figure 1C, [25]). In *Chlamydomonas*, *Tetrahymena*, *Paramecium* and human cells, Bld10 mutation or depletion lead to several CBB structural defects such as loss of some triplet MTs, triplet MTs misorientation in *Tetrahymena* and decrease of the spoke length in *Chlamydomonas* [14,21,25,27]. However, BLD10 is not essential for cartwheel formation in *Drosophila*, which suggests some degree of redundancy with other molecules [29,31].

The other protein that can link spokes to the MTs is CPAP/SAS-4. This protein localises at the centriolar lumen and wall in *Drosophila* and human cells and is essential for centriole duplication and elongation ([28-30] and reviewed in [32]). The N- and C–termini of CPAP directly bind to MTs and CEP135, respectively (Figure 1C, [25]), and SAS-4 is essential for cartwheel formation in *Paramecium* [33]. The 9-fold symmetry of the centriole also seems to depend on another daughter centriole component, SAS-5/Stil/Ana2. This centriolar protein is essential for centriole duplication in several organisms including *Drosophila*, *C. elegans*, zebrafish and mammals ([6,34-37] and reviewed in [32]). Moreover, SAS-5 interacts directly with SAS-6 in *C. elegans* and *Drosophila*, and indirectly via CPAP in human cells [34,35,38], and they depend on each other for their centriolar localisation [35,38]. Interestingly, overexpression

of SAS-6 and Ana2/SAS-5 in *Drosophila* leads to the formation of cartwheel-like structures [34]. In *C. elegans*, two models for centriole assembly have been recently proposed. In Model I SAS-6 interacts with SAS-5 to form an array of 9-fold symmetric cartwheel spokes [26], whereas in Model II a spiral array of SAS-6 oligomers alone forms a central tube and establishes the 9-fold symmetry [39] (for more details see Figure 1B and its legend).

Centriole formation, elongation and maturation

A mystery surrounding centriole growth is their incredible stability through several cell divisions and the constancy of their length within a cell type, once their growth is finished. In most organisms new centrioles assemble and start elongating in S-phase, followed by elongation of distal region through the G2 and M phases. Novel imaging techniques brought new ultra-structural details to the mechanisms of procentriole formation. While data based on conventional transmission electron microscopy on the BBs of *Paramecium* suggested that A-, B- and C-tubules are added sequentially from the proximal to the distal end [5], cryo-electron tomography data from human centrioles suggests that the A-tubule is first nucleated proximally by a γ-tubulin ring complex -like structure followed by the addition of B- and C-tubules at different lengths [10] (Figure 2A). Although cartwheel structures were not investigated in this study, the near-native 3D density map of the *Chlamydomonas* BB revealed the organization of all triplet MTs, linkers (between either two adjacent tubules of the triplets or consecutive triplets) and additional non-tubulin densities whose protein composition remains mostly unknown [40,41] (Figure 1D). The linkers connecting the adjacent triplet MTs and the structures extending towards the lumen from the triplet MTs, present at the cartwheel free region of the BB, are possibly stabilizing the entire BB barrel [40]. Interestingly, in *Chlamydomonas* BB the proximal and distal organisations are significantly different, suggesting that centriole biogenesis is a sequential process perhaps linked to specific cell cycle stages [40].

A variety of conserved molecular players identified recently suggest at least two mechanisms to control centriole growth: i) a balance between MT polymerization and depolymerisation, a consequence of the antagonistic functions of a MT depolymerase (KLP10A) and nucleators/stabilisers (e.g. CPAP, CEP120, Spice1, Centrobin, OFD1, Poc1) and ii) the presence of a centriole cap that restricts growth (e.g CP110-CEP97) ([42,43] and reviewed in [44,45])

(Figure 2A and B). How these molecules play together to define centriole length is not yet known.

While new centriole formation and elongation require one cell cycle, its maturation occurs only during the following cell cycle [44]. This step is characterised by the acquisition of the aforementioned sub-distal and distal appendages, which are thought to be the homologous of the BB appendage-like structures, basal feet and transitional fibers, respectively (ODF2 paper Tateishi, JCB, 2013) . Indeed, the sub-distal appendages harbour MT anchoring and nucleating proteins, e.g. CEP170, ε-tubulin and ninein [44], and distal appendages contain several proteins essential for cilia formation such as CEP164, CEP162 and CEP123 ([46,47] and reviewed in [1,44]). The roles of these structures in cilia assembly and symmetry establishment are discussed in the following section.

Cilium compartments and their organization

The cilium can be divided into two compartments: 1) the transition zone (TZ) linking the BB to the cilium, and 2) the axoneme. The latter is divided into two zones: the doublet MT zone mostly characterized by the presence of motility-associated protein complexes in motile cilia and the distal singlet MT zone including the ciliary tip structure (Figure 3). Based on the MT architecture, axonemes are generally classified into three types: i) '9 + 2' (9 doublets MTs, with dynein arms, radially arranged and a central pair of singlet MTs) cilia are generally motile, ii) '9 + 0' with dynein arms (9 doublets MTs radially arranged and no central pair of MTs) are usually motile cilia and iii) '9 + 0' without dynein arms (9 doublet MTs radially arranged and no central pair of MTs) are usually immotile cilia (Figure 3). Although, the 9-fold symmetry is common to both CBBs and cilia (Figure 3 and [48]), several components are exclusive to either CBB or cilia, e.g. motility associated components are only present in the cilia while most proteins involved in centriole biogenesis are exclusively present at the CBB [16,49,50]. These observations raise several interesting questions. How are the 9-fold symmetry, length and stability of both structures regulated? Here, we will discuss these questions in the context of the organization mechanisms of TZ and doublet MT zone.

Transition zone components and their organization

The TZ is a specialized compartment that varies in structure, length and molecular organization between different organisms. This compartment is found at the base of cilium where doublet MTs are heavily cross-linked to the surrounding ciliary membrane (Figure 3; [51-53] and reviewed in [9]). Recently, many human disease-associated proteins were found to localize to the TZ, therefore raising important questions about its assembly and function [1,9]. Interestingly, perturbation of TZ proteins induces defects either in BB docking to the plasma membrane or in the formation of Y-linkers, Y-shaped connections between the axonemal MTs and the ciliary membrane, disrupting cilia assembly and/or ciliary trafficking [9,47,54]. Although little is known about the molecular organization of the TZ, recent studies described that at least three distinct modules (NPHP1-4-8, NPHP5-6, and MKS) interact to form the TZ in mammals. Until now, only two of these modules (NPHP1-4 and MKS-MKSR) are described in *C.elegans* suggesting diversity in TZ composition. Nevertheless, studies from *C. elegans*, zebrafish and mammalian cells show that several of the TZ components as well as their interactions are common between different organisms [53,55-57], suggesting a partially conserved mechanism of TZ assembly.

Briefly, the interaction between CEP164, a distal appendage protein, Rabin8 and Rab8 GTPase regulates the vesicular trafficking to the centriolar distal appendages, an event required for the docking of the BB to the plasma membrane (Figure 4A, [54]). Subsequently, CEP162, another distal end centriolar protein, binds to MTs at the TZ and recruits TZ proteins of the three different modules, such as NPHP1-4-8, CEP290/NPHP6 and MKS/B9 [47]. Of these, CEP290/NPHP6 localizes in between MT and ciliary membrane, where it interacts with several other TZ localizing proteins, such as BBSome, NPHP5 and BBS6 [47,55,58]. The loss of CEP290 function prevents Y-linker assembly in *Chlamydomonas* and mouse photoreceptor cells (REF.). Altogether, these suggest CEP290 may act as an anchor in the formation the TZ cross-linkers, which may regulate the protein traffic into cilia (for details see Figure 4Ab). Although these studies have begun to elucidate the mechanism of TZ assembly, most of the TZ components´ functions, interactions and structural organization remain unknown. The use of cryo-electron tomography and super-resolution imaging techniques will help elucidating the molecular mechanism of TZ assembly, organization and function. Recent studies propose the existence of

an additional ciliary segment distal to the TZ, called “inversin compartment”. Although few proteins localize there, e.g., inversin/NPHP2, NEK8 and NPHP3, the role of this zone remains to be understood.

Doublet MT zone organization and functional implication in motile cilia

Doublet MTs and their associated structures: The doublet-MT zone is the most studied ciliary compartment due to its abundance and its contrasting features between motile and immotile cilia (Figure 3). The recent near-native structures of the *Chlamydomonas* flagellum confirmed previous knowledge and revealed several new structures: i) each doublet MT contains a complete A-tubule (13 protofilaments), fused to an incomplete B-tubule (10 protofilaments) through novel non-MT periodic structures [59,60], ii) other newly identified non-MT periodic structures, the MT inner proteins, present on the inner wall of the doublet MTs and proposed to ascertain doublet MT stability and length regulation [59-61]. Though the molecular nature of these non-MT structures is unknown, similar features also exist in the A- and B-tubules of *Chlamydomonas* and *Trychonympha* BB [16,40], suggesting an unknown common mechanism of assembly and stabilization of A and B-tubules in CBB and cilia.

For instance, Kinesin-13, a conserved MT depolymerising motor, is implicated in both centriole and cilia length control (Figure 4B), supporting the above mentioned hypothesis. While *Drosophila* kinesin-13 (KLP10A) depolymerises centriolar MTs [62], *Giardia*, *Trypanosoma* and *Chlamydomonas* kinesin-13 depolymerise axonemal MTs [63-65]. In addition, *Chlamydomonas* kinesin-13 (CrKinesin-13) depolymerises cytoplasmic MTs providing tubulin precursors for axoneme assembly [65,66]. Together these observations suggest the existence of similar mechanisms regulating centriole and cilia length which need further investigation. Mapping the molecular composition of MT inner proteins and non-MT structures associated to the doublets and further investigation on their functions in axonemal MT assembly and stability will be very important to understand cilia formation and maintenance.

Motility associated structures: The fundamental unit of the ciliary axoneme is a 96 nm repeat structure (Figure 4C) along its length that usually consists of at least four different types of structures essential for cilia motility: i) outer dynein arms, ii) inner dynein arms, iii) the nexin–dynein regulatory complex, iv) three radial spokes (RS) that project toward the central pair

complex (CPC) and interact with a calmodulin and spoke-associated complex (Figure 4C; [59,61,67]). The dyneins (outer and inner dynein arms) and dynein-associated complexes are crucial for the axonemal doublet MT bending during cilia movement (for detail reviews see [68,69]). In addition, the RSs, essential structural components of the axoneme, act as mechano-chemical transducers between the CPC and the peripheral doublet MTs in *Chlamydomonas*. Since the structures and functions of the axonemal dyneins and dynein-associated complexes are described elsewhere [69-71], we restrict our discussion to the structural organization and functions of RSs and CPC.

The *Chlamydomonas* RSs, composed of at least 23 proteins, are ~43 nm long T-shaped structures. The recent near-native 3D ultra-structures of *Chlamydomonas* axoneme revealed that RS can be divided into four distinct domains: i) a short base, anchored to the protofilaments A12 and A13 of doublet MTs, ii) a long stalk, iii) a variable bifurcated neck, and iv) an orthogonal head, which connects to CPC (Figure 4C). Comparative analysis between the 3D ultra-structures of wild type and mutants (e.g., *pf1*, *pf14*, *pf17*, *ida4* etc.) axonemes suggest these morphological subdivisions exhibit different protein compositions in *Chlamydomonas* [72,73]. For example, in the *pf1* mutant axoneme, the Radial Spoke Proteins (RSP) 1, 4, 6, 9 and 10 are absent, and both RSs (RS1, 2) lack very similar plate-like structures, which usually extend perpendicular to the RS stalk at the distal end of the RSs [72]. Similarly 3D-cryoET of WT and mutants of *Chlamydomonas* axonemes helped mapping the components and organization of all motility associated complexes in the axoneme (for more detail see [72,73]). For instance, the components of the four sub-domains of RS1 and 2 are as follows: i) the short base is composed of calmodulin (CaM), and CAM-IP2-4 ii) the long stalk is composed of RSP3, 5, 7, 8, 11-15 and 17-22, iii) the bifurcated neck is made of RSP2, 16 and 23, and iv) RSP1, 4, 6, 9 and 10 form the orthogonal head [72]. Moreover, while most organisms (*Tetrahymena*, *Paramecium*, *Trypanosoma* and sea urchin) contain three spokes (RS1, RS2, and RS3), *Chlamydomonas* and *S. bullata* contain only pairs of spokes (RS1 and RS2) within the axonemal repeat unit. Proceeding from the proximal to the distal axonemal end, RS1 is the first in each triplet. RS2 and RS3 are about 32 and 56 nm distal to RS1, respectively [72,73]. While RS1 and RS2 are grossly similar looking structures with little morphological differences in *Chlamydomonas*, *Tetrahymena* and

sea urchin, RS3 is morphologically distinct from RS1 and RS2 in *Tetrahymena* [61]. In addition to the significant variability in the periodicity and size of the RSs, the structural variability in dyneins and DRCs in *Chlamydomonas*, *Tetrahymena* and sea urchin may explain differences in their cilia motility [61]. Interestingly, recent biochemical analysis highlighted interactions among different RSPs, e. g. RSP4 and RSP6 independently binds to both RSP9 and RSP10 [74]. Together with the 3D-utrastructural analysis of several *Chlamydomonas* RSP mutants, these interaction data provide insights on the RS subunits organisation and consequently on the mechanism of RS assembly, which may also be partly conserved in diverse organisms [72]. In the cell body, at least 11 RSPs (RSP1-7 and 9-12) form a "7-shape" 12S soluble complex which is transported into the cilia [75]. Subsequently, this precursor interacts with the remaining 12 RSPs to form the 20S RS complex, proposing a stepwise assembly mechanism of RS in axoneme [75]. In contrast, during axoneme maintenance and disassembly, the full 20S RS complex is transported back to cell body, where the complex disassembles to form 12S complex [76]. However, little is known about the assembly mechanism of RSP8, 13-23 and their interaction with 12S to form a complete RS.

Another interesting structure is the CPC, which is composed of a central pair of MTs and associated non-MT structures, and is essential for coordination of cilia motility [11,77]. The 3D structure of the CPC shows the presence of connections between : 1) the two central MTs, 2) the CPC projections, and 3) the central MTs and the CPC projections [78]. Although the molecular composition of these connections remains unknown, they seem to play a critical role in transmitting the structural and chemical signals from the CPC to the outer doublet MTs through the RSs. [61,79]. Interestingly, the central pair of MTs may twist upon flagella beating only in some species [61], reinforcing the orchestrated but evolutionary plastic functions of many motility-regulator complexes, including CPC, RS, and dyneins [69]. Nevertheless, biochemical studies of the interaction between RSs and the CPC and their near-atomic structures are still required to fully understand the role of RSs and CPC in axoneme motility regulation.

Collectively, these studies suggest the most important attributes conferring motility to axonemes are the presence of the dynein arms on the doublet MT and CPC. Studying the 3D

morphology of the different near native immotile and motile cilia will further clarify cilia assembly and motility.

Perspectives

During the last five years, cryo-electron tomography led to an unprecedented 3D ultra-structural comparative view of CBB and axoneme organization [10,15,16,40,59-61]. The presence of common features in the CBB and axoneme, such as A- and B-tubules, MT inner proteins and non-MT connections between adjacent MTs, suggests similar assembly and elongation mechanisms [40,59]. Indeed, Kinesin-13, a MT depolymerase, regulates both CBB and axoneme length [62,65,66]. Though, CBBs and axonemes share many common features, many differences in their non-MT structures and composition, such as the presence of the cartwheel in CBBs and the motility apparatus in axonemes, are also observed [49,50,80]. Biochemical, genetic and structural studies have helped to unravel the molecular composition of those structures [16,23-25,67,69]. Those components are present only in organisms having CBB/cilia suggesting the conservation of a specialized molecular machinery essential for their assembly [2,31]. Further studies on those structures and others within CBBs and cilia will help to understand how they lead to the different functions of CBBs and axonemes. For instance, despite knowing many CBB and TZ localizing proteins [50,55,57], lack of detailed biochemical interaction mapping and near-native 3D structural data prevents the construction of molecular maps of the non-cartwheel part of CBB and the TZ. Finally, the observed diversity of structures, such as the cartwheel and TZ, between organisms [6,10,16,40,61], suggests a plasticity in the assembly mechanisms leading to different functions. The time has come to expand high resolution structural studies to mutants affecting CBB/cilia elongation and stability to decipher the molecular mechanisms of CBB and axoneme assembly and how they impinge in function.

Figure Legends:

Figure 1: Organization and Construction of CBB. A, B) Schematic representation of longitudinal and cross sections of the "canonical" mother-daughter centriole pair in most animal cells (**A**) and in *C. elegans* (**B**). (**A**) Generally, the daughter centriole is composed of 9 radially arranged MT triplets (A-, B- and C- tubules), forming a cylinder (for more details see the text) [1]. (**B**) Schematic illustration of the *C. elegans* centriole and cartwheel. The mother centriole in *C. elegans* is composed of 9 radially arranged MT singlets (A-tubules), which assemble around a ~150 nm long cylinder of >100nm in diameter. The cylinder is probably built around a cartwheel like structure. The daughter centriole forms orthogonally from the mother centriole. At early stages, the length (<60 nm) as well as the diameter (<100nm) of the cylinder are shorter than those of the mother centriole [6]. The inner layer of the central tube is formed by SAS-6 and SAS-5, while the outer layer is built by SAS-4, which interacts with MTs. Two distinct models are proposed for the establishment of the 9-fold symmetry. Model I refers to the formation of a typical cartwheel composed of ring stacks, whereas model II supports the existence of a double spiral of SAS-6 [26,39]. (**C**) (**a**) Schematic representation of the proximal end of the cartwheel with its associated proteins, based on cryo-electron tomography of *Trichonympha* BB [15,16]. (**b**) 3D longitudinal representation of a cartwheel segment (right). Each layer consists of two ~22 nm diameter central rings ~8.5 nm apart joined by their spokes at the periphery, therefore generating a ~17-nm periodicity at the margin. (**c**) A close-up view of the A-tubule and its associated proteins (right below) obtained by applying a 90° rotation of the view presented on the left. CEP135 localizes at the pinhead of the cartwheel and serves as a bridge between the spokes and the outer MTs (possibly the A-tubule). This property is mediated by direct interactions of CEP135 with SAS-6 (via its C-terminal domain), MTs and SAS-4 (via its N-terminus) [25]. **D**) 3D schematic representation of the "canonical" mother centriole in most animal cells [40,41] Proximal and distal (mirror imaged) views of the 3D reconstructed *Chlamydomonas* BB model. MT triplets are represented in blue and non-tubulin associated proteins in yellow. Note the structural differences between the proximal and distal regions of the BB at the level of the C-tubule and non-tubulin structures (arrow marked). Black arrowhead - indicate changes in the non-MT structures. Distal view is mirrored to facilitate the comparison with proximal view [41]. **E**) Lengths of Full, C-terminal and Coiled-coil domains of SAS-6 of

different organisms. The predicted maximum length of SAS-6 coiled-coil domains was calculated by multiplying the number of residues by 0.1485 nm (axial rise per residue). The approximate distance between the hub and the A-MT was measured from electron micrographs available in the literature. NM- not measured.

Figure 2: Mechanisms of CBB assembly. Model presentation of procentriole assembly in most animal cells (A) and *C. elegans* (B) [6,10]. A) (**i- iii**) The first step of procentriole assembly involves the formation of a stalk and the central hub of the cartwheel at the proximal end of the mature centriole (**i**). In most animal cells, procentriole formation requires CEP152-dependent PLK4 localisation at pre-existing centrioles. (**iii**) The cartwheel assembles and organises the procentriolar wall, in which some A-MTs start growing from the γ-tubulin ring complexes. PLK4 is in turn required for SAS6 and STIL recruitment and maintenance at centrioles. (**iv-viii**) Only the procentriole shown in (**iii**) and daughter centriole grown from it is presented. (**v**) Before completion of the 9 A-tubules, some B-tubules start growing from their walls. (**vi**) B-tubules grow bidirectionally, and C-tubules start growing from their walls [10]. (**vii**) C-tubules grow bidirectionally until B- and C-tubules reach the proximal end of the A-tubule. SAS-6 and SAS-5, whose localization at the centriole is thought to be interdependent, are essential for SAS-4 recruitment to the centriole, with the latter being thought to induce MT incorporation to centrioles along with γ-tubulin. (**viii**) Growth continues at the distal end until completion of the MT triplet blades. Subsequently, elongation of the newly formed centriole is promoted mostly by SAS-4, CEP120, and CEP135, and restricted by CP110-Cep97 [10,31,42,45]. (B) (i, ii) An initial 60-nm long central tube, <100nm in diameter, is formed with a perpendicular orientation to the wall of the pre-existing centriole. SPD-2 and ZYG-1 are recruited to the mother centriole, before daughter centriole assembly. SPD-2 is required to recruit ZYG-1 to mother centrioles. Both SPD-2 and ZYG-1 are required for the recruitment of the SAS-6 and SAS-5, coincident with the formation of the daughter centriole central tube (ii, iii). SAS-5 and SAS-6 are required for SAS-4 recruitment. The central tube elongates during pronuclear migration, and singlet MTs assemble around it during pronuclear rotation in a SAS-4 dependent fashion to form a fully elongated daughter centriole (iii, iv). Finally, the central tube diameter

and length increase concurrently with SAS-4 mediated singlet MT assembly around its circumference (iv, v) [6].

Figure 3: Schematic presentation of the cilia structure. (**a**) Longitudinal view of the skeleton of the cilium/flagellum which grows from the distal part of the BB. In many BBs, the centriolar cartwheels (**b**) are retained and required for BB stability. The distal part of the BB is called the transition zone, and starts where the outer C-tubule of the triplet stops growing. During centriole to BB differentiation, the acquisition of specialized structures, such as transitional fibers (**c**), provides mechanical support to the cilia, serving as platforms for the docking of ciliary components. The Y-linker structures linking the doublet MTs to the ciliary membrane provides rigidity to the cilia and generate a mesh like structure at the base of the cilia (**d**). The axoneme, the MT skeleton of cilium, is divided into two zones, the doublet and the singlet MT zones. (**e, f**) The doublet zone contains either only 9 peripheral MT doublets (in most immotile cilia) or 9 peripheral MT doublets with dynein arms and a central MT pair (in most motile cilia). While in *Chlamydomonas* the two MTs of the central MT pair start growing simultaneously from the distal part of the TZ, in *Drosophila* a singlet MT extends from the BB lumen to template the central MT pair (cyan and green tube with dotted border) (c-c', d-d' and e-e') [11]. (**g**) In the singlet MT zone, B-tubule of the doublet MT stops growing and A-tubules gradually terminate. This region is highly variable in size, very small in *Chlamydomonas* and long in many *C. elegans* and *Drosophila* bipartite sensory cilia [81-83].

Figure 4: Schematic presentation of cilia assembly mechanism and structure of the doublet MT zone of the axoneme. (**A**) (a) Mother centrioles acquire appendages and recruit proteins like Centrosomal protein of 290 kDa (CEP290, also called NPHP6) and Meckel syndrome, type 1 (MKS1). CEP290 recruitment to the centriole distal part is regulated by peri-centriolar material 1 (PCM-1) and Bardet–Biedl syndrome protein 4 (BBS4)[58,84]. CEP290, MKS1 and BBS4 are mutated in Nephronophthisis, Meckel–Grueber syndrome and Bardet–Biedl syndrome, respectively [1]. Golgi-derived vesicles, which are rich in Rab8 and Rabin8, dock to the mother centriole appendices through the interaction with Centrosomal protein of 164 kDa (CEP164),

leading to the encapsulation of the distal part of the centriole by membrane, followed by initiation of the axonemal growth within the encapsulation [54]. At this time, CP110 is removed from centriole and Centrosomal protein of 162 kDa (CEP162, an axoneme recognizing protein) is recruited to newly made transition zone TZ, followed by fusion of the modified mother centriole to the plasma membrane. Then CEP162 recruits many proteins of the three TZ modules, such as NPHP1-4-8, NPHP6/CEP290 and MKS, essential for cilia assembly. Intraflagellar transport (IFT) components are involved in transporting molecules in and out of the cilia and are also mutated in ciliopathies, such as cytoplasmic dynein 2 heavy chain 1 [1]. (b) Schematic presentation of few TZ proteins organization based on their known interactions with CEP290. (**B**) Schematics diagram of the regulation of centriole and cilia length. Kinesin-13, a MT depolymerase, regulates the centriole length in *Drosophila* [62] (**a**) and cilia length in *Chlamydomonas* and human cells [85] (**b**). In *Chlamydomonas*, CrKinesin-13 regulates both the cilia assembly by depolymerising the cytosolic MTs to provide tubulin precursors, which are transported into cilia by anterograde intra flagellar transport (IFT) and cilia disassembly by depolymerising the axonemal MTs, followed by retrograde IFT [66]. Conservation of these mechanisms needs further investigation. (**C**) (a) Scheme of the 9 + 2 axonemal structure, showing the position of the main axonemal components: Radial spokes (orange), inner dynein arms (IDA, blue), outer dynein arms (ODA, red), microtubules (gray), Dynein regulatory complex (green), central pair complex (black). (b) Cross-sectional view of the proximal region of the axoneme showing the different RSs domains: base (orange), stalk (green), neck (blue) and head (red). (c) Longitudinal view of the proximal end of the *Tetrahymena* and *Chlamydomonas* axoneme. For simplicity, only the RSs and the A-tubule are represented. The RS3 stump (RS3S) observed in *Chlamydomonas* is depicted in orange while the RS3 observed in *Tetrahymena* is represented in yellow.

Figure 1:

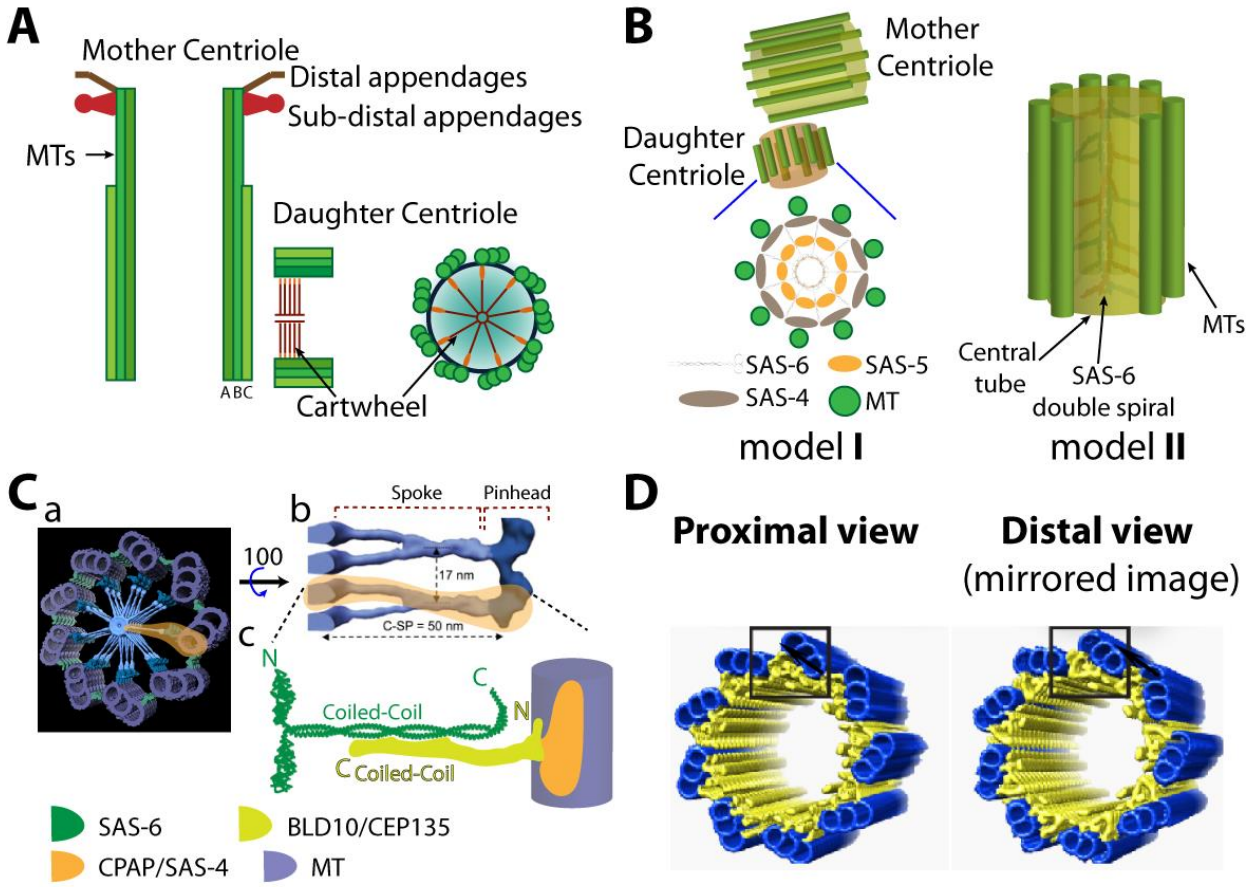

E

	SAS-6					Hub to MT distance
	Full length (aa)	Globular C-terminal length (aa)	CC domain (aa)	Length of CC domain (aa)	Length of CC domain (nm)	
Danio rerio	627	133	165-494	329	48,9	60-70
Homo sapiens	657	186	162-471	309	45,9	NM
Chlamydomonas reinhardtii	728	225	180-503	323	48,0	70
Tetrahymena thermophila	703	153	217-550	333	49,5	70
Trichonympha agilis	531	56	186-475	289	42,9	70
Drosophila melanogaster	472	39	171-433	262	38,9	70
Paramecium Aurelia	591	65	180-526	346	51,4	70
Caenorhabditis elegans	492	89	192-403	211	31,3	30 (daughter) - 50 (mother)

Figure 2:

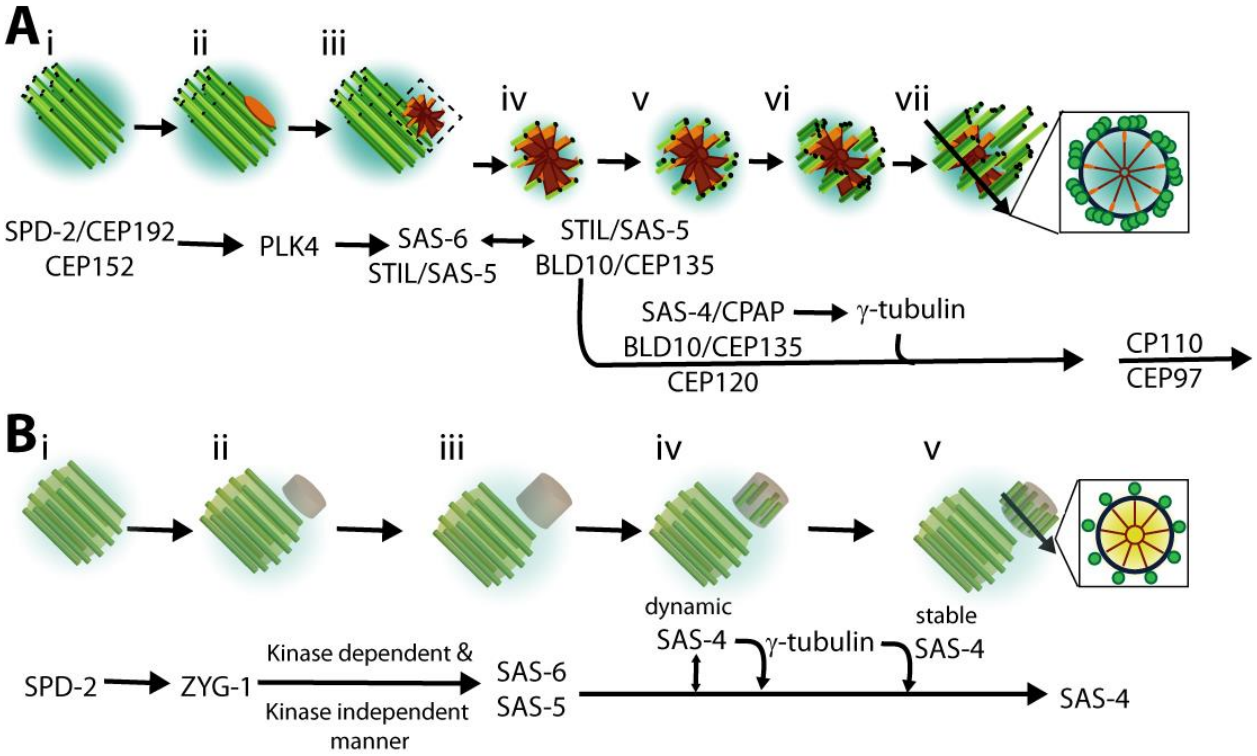
A
i
ii
iii
iv
v
vi
vii
SPD-2/CEP192
CEP152
PLK4
SAS-6
STIL/SAS-5
STIL/SAS-5
BLD10/CEP135
SAS-4/CPAP
γ-tubulin
BLD10/CEP135
CEP120
CP110
CEP97
B
i
ii
iii
iv
v
dynamic
stable
SPD-2
ZYG-1
Kinase dependent &
Kinase independent
manner
SAS-6
SAS-5
SAS-4
γ-tubulin
SAS-4
SAS-4

Figure 3:

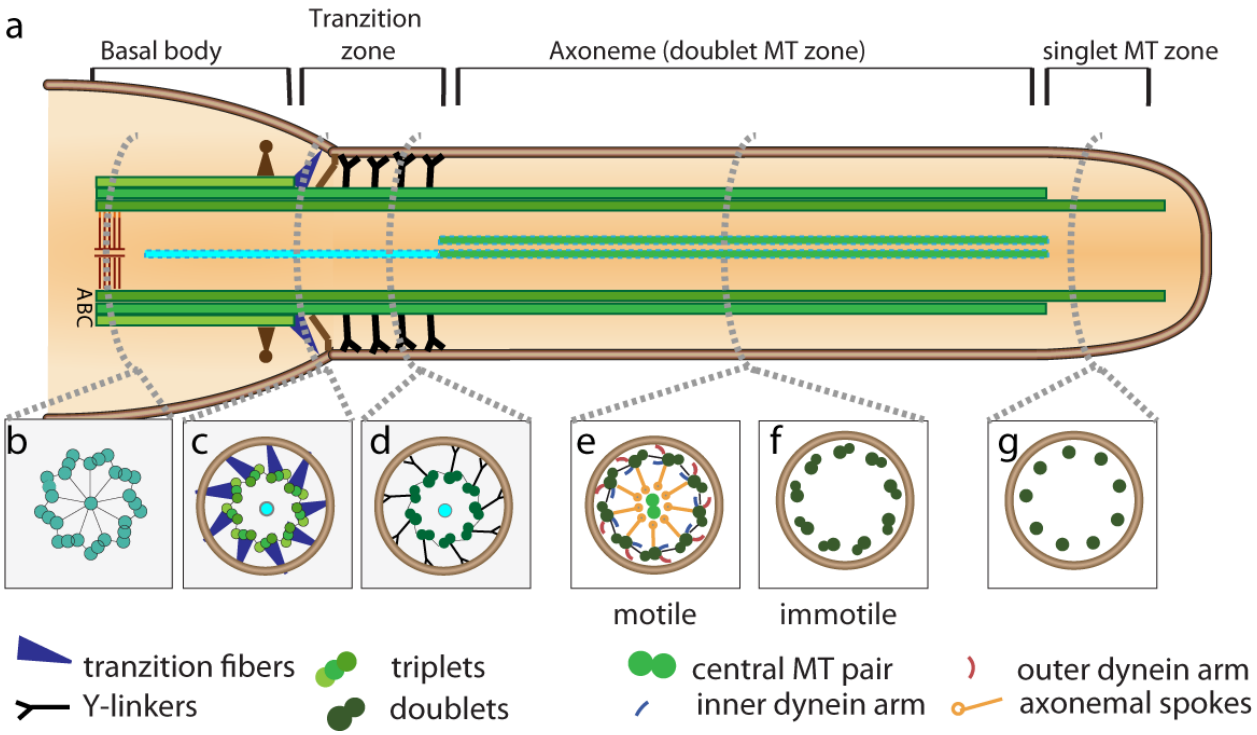
a
Basal body
Tranzition zone
Axoneme (doublet MT zone)
singlet MT zone
ABC
b
c
d
e
f
g
motile
immotile
tranzition fibers
Y-linkers
triplets
doublets
central MT pair
inner dynein arm
outer dynein arm
axonemal spokes

Figure 4:

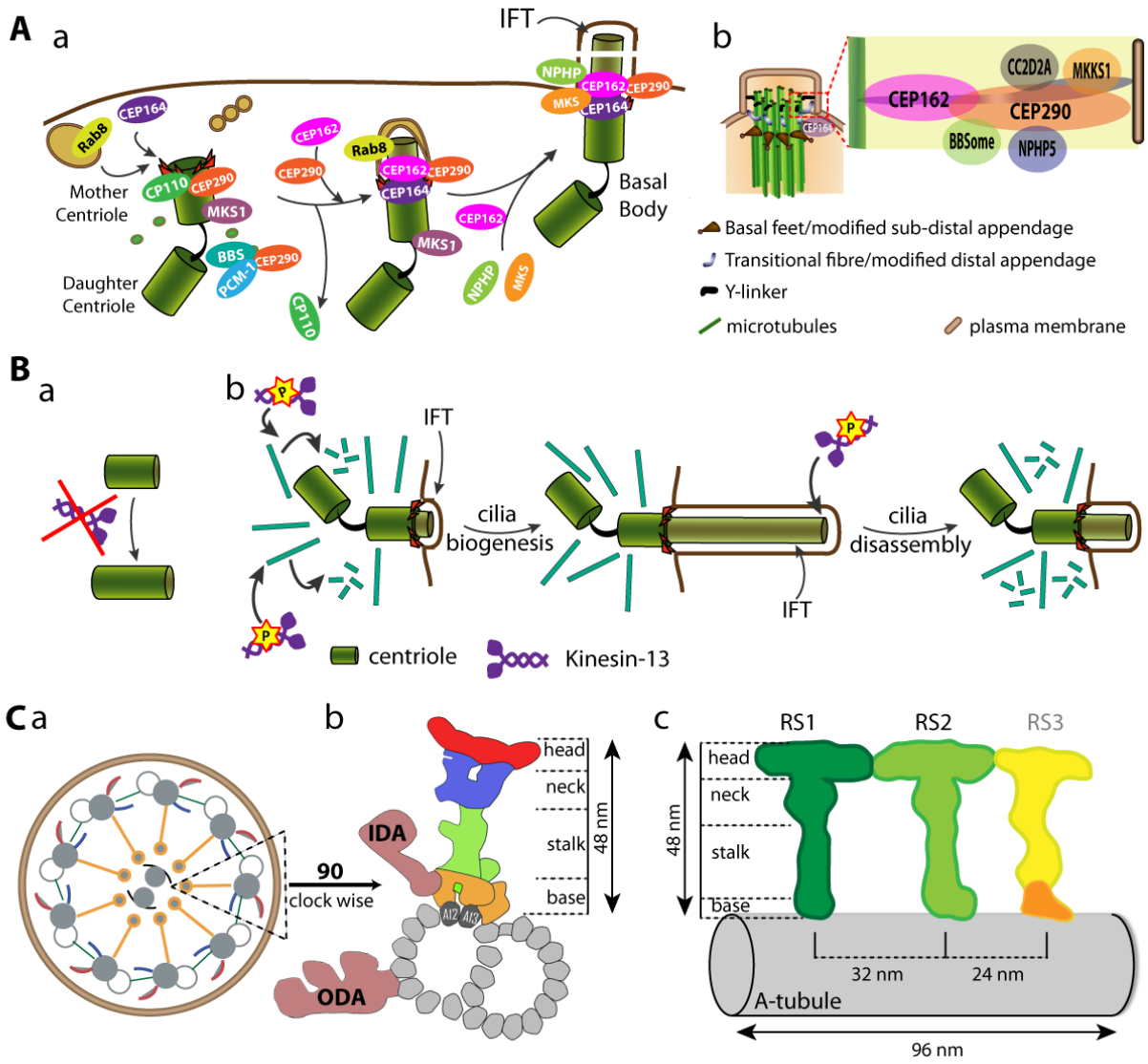
A
a
IFT
Rab8
CEP164
Mother Centriole
CP110
CEP290
MKS1
BBS
PCM-1
Daughter Centriole
CEP162
Basal Body
NPHP
MKS
b
CC2D2A
MKKS1
CEP162
CEP290
BBSome
NPHP5
Basal feet/modified sub-distal appendage
Transitional fibre/modified distal appendage
Y-linker
microtubules
plasma membrane
B
a
b
P
IFT
cilia biogenesis
cilia disassembly
centriole
Kinesin-13
C
a
b
90
clock wise
IDA
ODA
head
neck
stalk
base
48 nm
c
RS1
RS2
RS3
32 nm
24 nm
A-tubule
96 nm